

On the Invariant Reactions in the Mo-Rich Portion of the Mo-Si System

Carlos Angelo Nunes, Gilberto Carvalho Coelho, and Alfeu Saraiva Ramos

(Submitted 16 June 2000; in revised form 16 March 2001)

The Mo-Si system presents two invariant reactions (eutectic and peritectic) in the Mo-rich region; these reactions involve the Liquid, Mo_{ss} , Mo_3Si , and Mo_5Si_3 phases. The results presented in the literature show disagreement about the specific reactions, with two proposals being reported: (1) $\text{L} + \text{Mo}_{\text{ss}} \rightleftharpoons \text{Mo}_3\text{Si}$ and $\text{L} \rightleftharpoons \text{Mo}_3\text{Si} + \text{Mo}_5\text{Si}_3$; and (2) $\text{L} + \text{Mo}_5\text{Si}_3 \rightleftharpoons \text{Mo}_3\text{Si}$ and $\text{L} \rightleftharpoons \text{Mo}_{\text{ss}} + \text{Mo}_3\text{Si}$. In order to contribute to this subject, we have produced several Mo-Si alloys (21 to 29 at.% Si) via arc melting and evaluated the as-cast microstructures through x-ray diffraction (XRD), scanning electron microscope/backscattered electron image (SEM/BSEI), and energy dispersive x-ray analysis (EDS). The primary phases identified in the different samples were Mo_{ss} , Mo_3Si , and Mo_5Si_3 . The results have indicated clearly the existence of a eutectic reaction involving the phases Mo_3Si and Mo_5Si_3 , confirming the existence of the $\text{L} + \text{Mo}_{\text{ss}} \rightleftharpoons \text{Mo}_3\text{Si}$ and $\text{L} \rightleftharpoons \text{Mo}_3\text{Si} + \text{Mo}_5\text{Si}_3$ invariant reactions. In addition, alloys with composition 26 at.% Si and 27 at.% Si presented Mo_3Si and Mo_5Si_3 as primary phases, respectively, indicating that the liquid eutectic composition is located between those values.

Introduction

The first study for the determination of the binary Mo-Si phase diagram was carried out by Kieffer and Cerwenka [1952Kie], and their proposed diagram is shown in Fig. 1. They proposed the eutectic $\text{L} \rightleftharpoons \text{Mo}_3\text{Si} + \text{Mo}_3\text{Si}_2$ and the peritectic $\text{L} + \text{Mo}_{\text{ss}} \rightleftharpoons \text{Mo}_3\text{Si}$ reactions in the Mo-rich region. In their study, the samples were prepared by hot pressing compacts from pure Mo and Si powders under an argon atmosphere. The samples were equilibrated in the temperature range of 1050 to 1800 °C and analyzed by x-ray diffraction (XRD), metallography, and melting point measurements. In a subsequent work, Nowotny *et al.* [1954Now] proposed the eutectic reaction $\text{L} \rightleftharpoons \text{Mo}_3\text{Si} + \text{Mo}_{\text{ss}}$ based on the existence of similar eutectics in the Cr-Si and W-Si systems and a peritectic reaction $\text{L} + \text{Mo}_3\text{Si}_2 \rightleftharpoons \text{Mo}_3\text{Si}$; the resulting phase diagram is shown in Fig. 2. The Mo_3Si_2 phase was better identified later as Mo_5Si_3 by Aronson [1955Aro], Dauben *et al.* [1956Dau], and Amberg [1960Amb], who also determined its crystal structure and lattice parameters. It should be pointed out that the work of [1954Now] did not involve experiments. Svechnikov *et al.* [1971Sve] carried out the most systematic study of this system, using XRD, metallography, and a high-temperature differential thermal analysis apparatus calibrated up to 2450 °C. They confirmed the invariant reactions proposed by Kieffer and Cerwenka [1952Kie], however, replacing the stoichiometry Mo_3Si_2 by Mo_5Si_3 . Figure 3 shows the Mo-Si phase diagram from the assessment of Gokhale and Abbaschian [1991Gok], who adopted the invariant reactions proposed by Svechnikov *et*

al. [1971Sve]. However, the studies of Christensen [1983Chr] and Arpacı and Froberg [1985Arp] were not considered in their assessment, where the suggested invariant reactions are as proposed by Nowotny *et al.* [1954Now], differing only by replacement of the stoichiometry Mo_3Si_2 with Mo_5Si_3 . The work of [1983Chr] involved crystal growth of the Mo_3Si and Mo_5Si_3 phases by the traveling solvent and Czochralski methods, respectively. This work on crystal growth supports the phase diagram shown in Fig. 2 by the fact that, during the growth from an alloy of composition 75Mo-25Si (at.%), the frozen zone in the last region to solidify was a mixture of Mo_3Si and Mo. The work of [1985Arp] was on the determination of mixing enthalpies of liquid Mo-Si alloys. His calculations of the liquidus line starting from pure Mo in the Mo-rich region support the phase diagram shown in Fig. 2. Considering these conflicting results, the aim of this work was to determine the actual invariant reactions taking place in the Mo-rich region of the Mo-Si system through the evaluation of the microstructures of several as-cast alloys with composition in the 21 to 29 at.% Si range.

Experimental Procedure

For this study, samples of nine Mo-Si alloys, each weighing approximately 5 g, were prepared by arc melting pure Mo (minimum 99.95 wt.%) and Si (99.999 wt.%) under pure argon (99.995%) in a water-cooled copper hearth furnace using a nonconsumable tungsten electrode. The silicon contents of the alloys varied from 21 up to 29 at.% Si. All alloys were melted five times to ensure chemical homogeneity. The mass losses during the processing of the alloys were lower than 0.3 wt.%. The as-cast Mo-Si alloys were characterized through XRD, scanning electron microscope/backscattered electron image (SEM/BSEI) and energy dispersive x-ray analyses (EDS). The XRD experiments were performed at

Carlos Angelo Nunes, Gilberto Carvalho Coelho, and Alfeu Saraiva Ramos, Faculdade de Engenharia Química de Lorena (FAENQUIL), Departamento de Engenharia de Materiais (DEMAR), Polo Urbo-Industrial, Gleba AI-6, s/n - 12600-000 - Lorena - SP - Brazil. Contact e-mail: cnunes@demar.fauenquil.br.

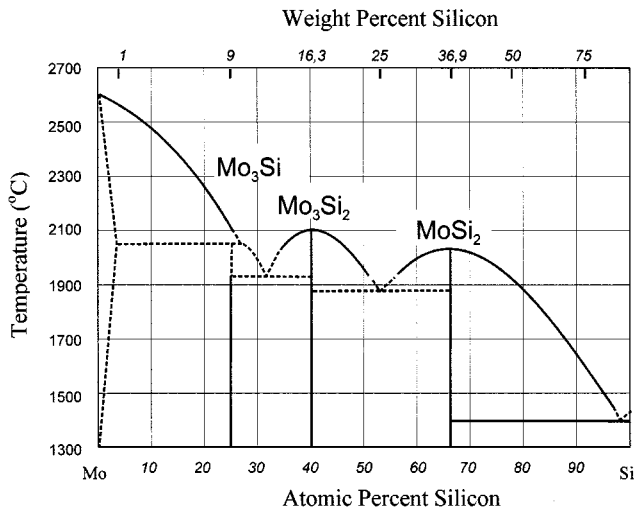


Fig. 1 Binary Mo-Si phase diagram from Kieffer and Cerwenka [1952Kie]

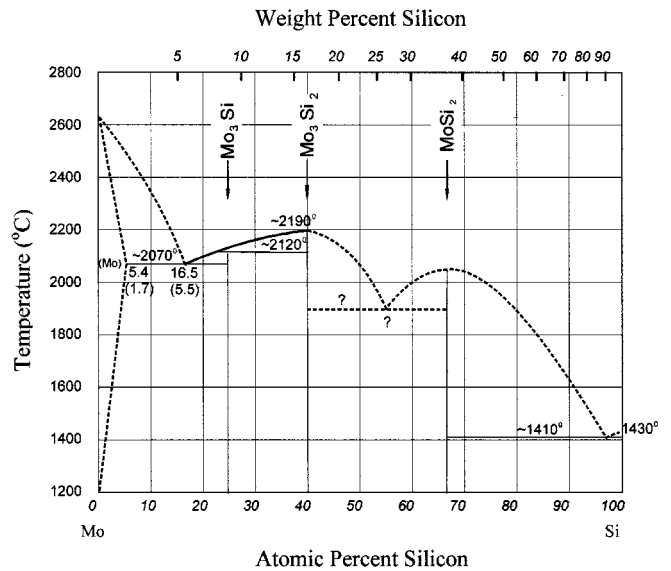


Fig. 2 Binary Mo-Si phase diagram from Nowotny *et al.* [1954Now]

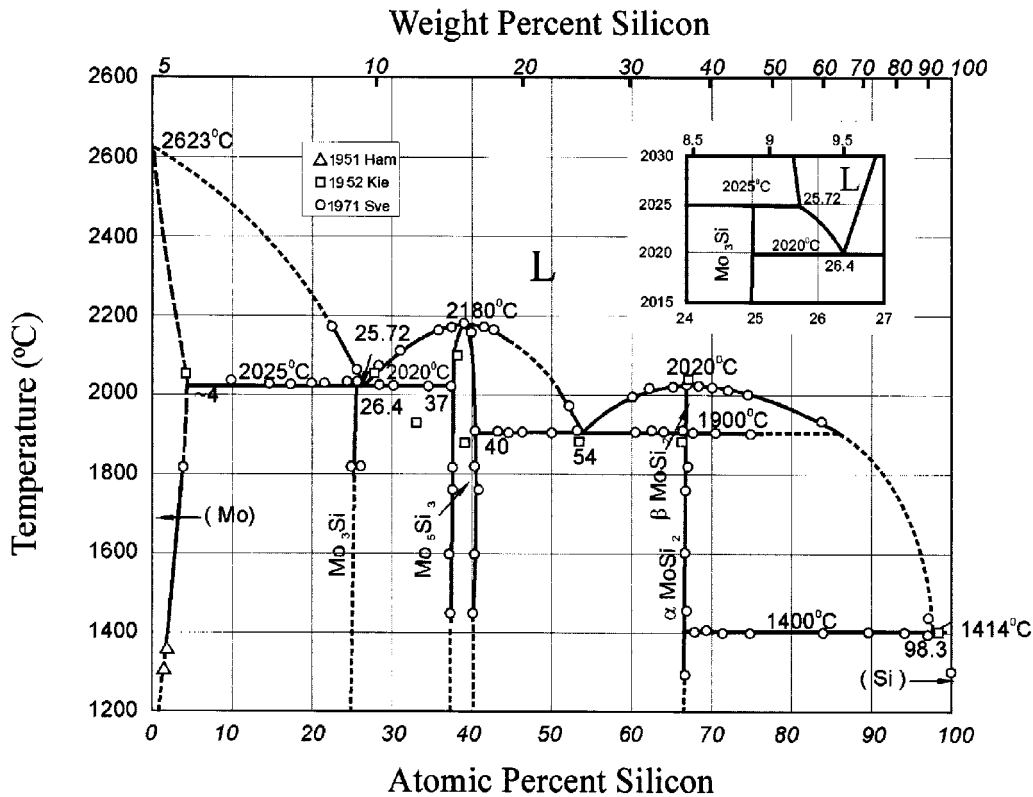


Fig. 3 Binary Mo-Si phase diagram from Gokhale and Abbaschian [1991Gok]

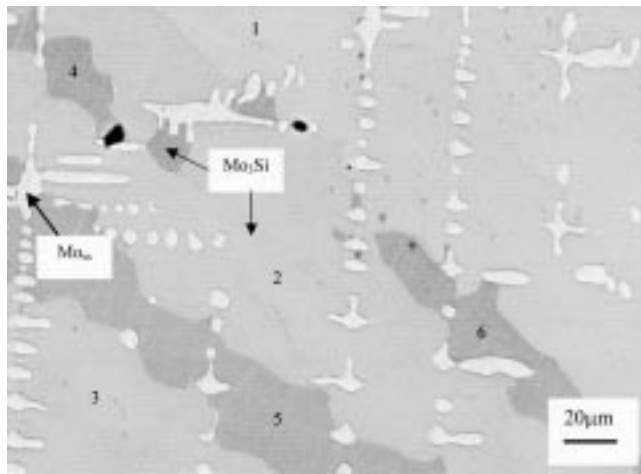
room temperature (Cu K_{α} radiation) from powders ($<177 \mu\text{m}$). The XRD patterns were indexed based on the JCPDS [1979JCP] database: Mo_{ss} (#4-0809), Mo_3Si (#4-0814), and Mo_5Si_3 (#34-871).

For the SEM analysis, the alloys were hot mounted, ground using silicon carbide grinding paper in the sequence #220 to #1000, and then polished with colloidal silica. The images were taken at 20 keV in the backscattered electron mode

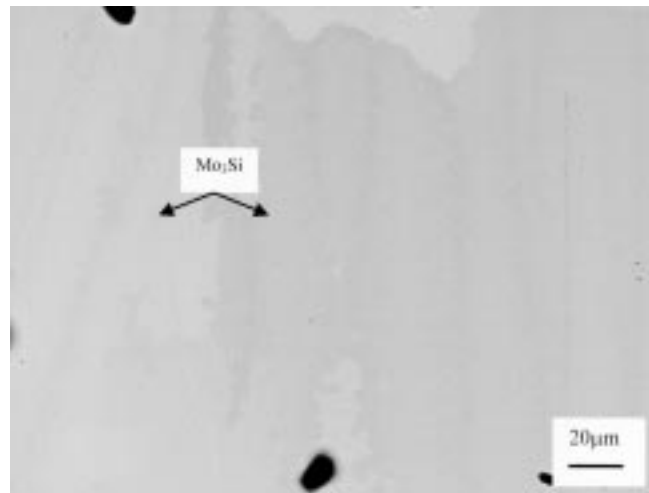
(BSEI) in a LEO Zeiss 1450VP SEM. The EDS standardless analyses were carried at 20 keV using the Mo L_{α} and Si K_{α} x-ray lines.

Results and Discussion

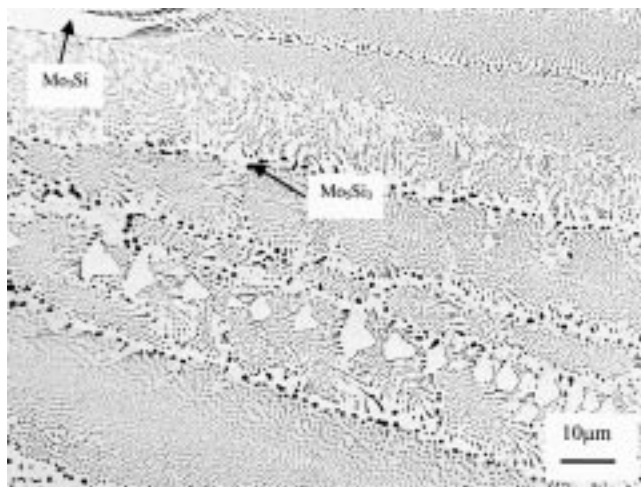
The $\text{Mo}_{79}\text{Si}_{21}$ and $\text{Mo}_{78}\text{Si}_{22}$ alloys presented similar microstructures. Figure 4(a) shows an SEM/BSEI micrograph of



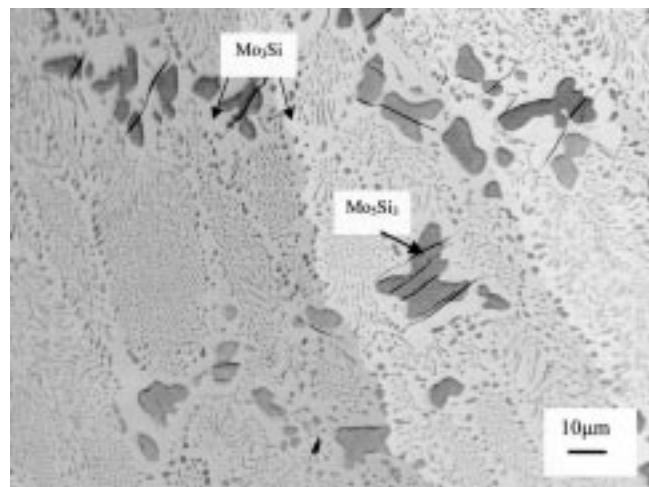
(a)



(b)



(c)



(d)

Fig. 4 Micrographs (SEM/BSEI) of as-cast Mo-Si alloys: (a) $\text{Mo}_{79}\text{Si}_{21}$, (b) $\text{Mo}_{77}\text{Si}_{23}$, (c) $\text{Mo}_{74}\text{Si}_{26}$, and (d) $\text{Mo}_{73}\text{Si}_{27}$. Numbers 1 to 6 in (a) indicate points of EDS analysis whose results are given in Table 1

Table 1 Results of EDS analysis from the Mo_3Si phase in the as-cast $\text{Mo}_{79}\text{Si}_{21}$ alloy. The points of analysis are indicated in Fig. 4(a)

Phase	Point of analysis	Mo (at.%)	Si (at.%)
Mo_3Si	1	80.4	19.6
	2	80.5	19.5
	3	79.9	20.1
	4	80.6	19.4
	5	80.0	20.0
	6	79.5	19.5

the $\text{Mo}_{79}\text{Si}_{21}$ alloy. Both alloys presented nonfaceted primary dendrites of the Mo_{ss} phase and the Mo_3Si phase filling out the interdendritic region, suggesting the occurrence of the peritectic reaction $L + \text{Mo}_{\text{ss}} \rightleftharpoons \text{Mo}_3\text{Si}$. This result is in agreement with Fig. 3, which indicates that the primary Mo_{ss} -phase precipitation region in the liquidus line extends up to 25.72 at.% Si. No sign of a eutectic reaction in these alloys

through SEM analysis was observed. It should be pointed out that the Mo_3Si phase may present different contrasts in a given BSEI micrograph, which is related to the crystallographic orientation effect of different grains on the SEM/BSEI contrast. Table 1 shows the results of the EDS analysis related to points 1 through 6 in Fig. 4(a). Note that the EDS results for the Mo_3Si phase gives a composition lower than 25 at.% Si. This error is likely associated to the use of standardless analysis; however, this value was used as a guide to identify the Mo_3Si phase in the different alloys. Figure 5(a) shows the XRD pattern of the $\text{Mo}_{79}\text{Si}_{21}$ alloy. Due to the low volume fraction of the Mo_{ss} phase in the microstructures and the overlapping of its most intense reflection associated to the (110) plane with the (210) plane of the Mo_3Si phase, the existence of the Mo_{ss} could not be confirmed based only on XRD data.

Figure 4(b) shows an SEM/BSEI micrograph of the $\text{Mo}_{77}\text{Si}_{23}$ alloy. Within the resolution of the observation, this alloy presented a Mo_3Si single-phase microstructure. As in the previous case, no sign of a eutectic reaction could be

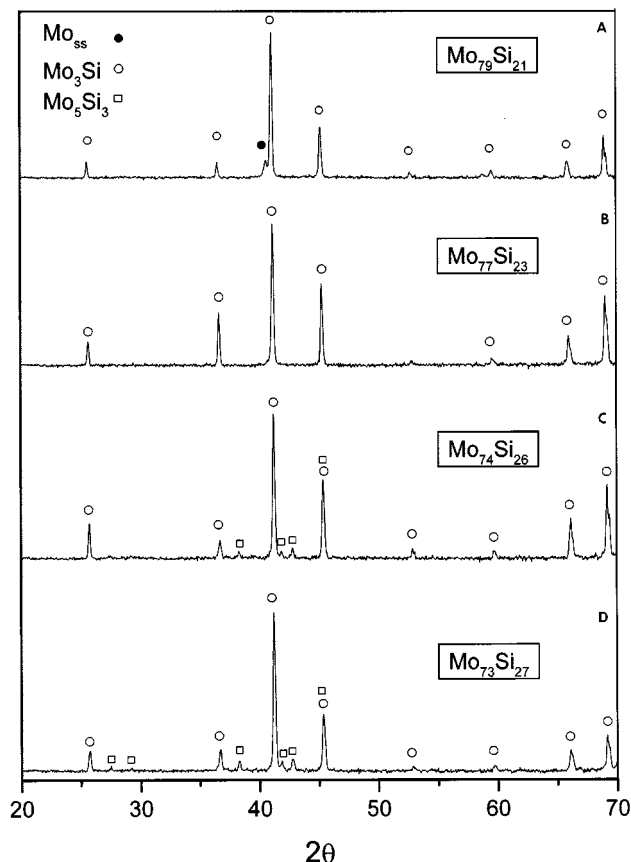


Fig. 5 XRD pattern of as-cast Mo-Si alloys: (a) $\text{Mo}_{79}\text{Si}_{21}$, (b) $\text{Mo}_{77}\text{Si}_{23}$, (c) $\text{Mo}_{74}\text{Si}_{26}$, and (d) $\text{Mo}_{73}\text{Si}_{27}$

observed. Based on the phase diagram shown in Fig. 3, this alloy should present a small amount of primary Mo_{SS} phase; however, the possibly existent Mo_{SS} crystals could have been consumed in the course of the $\text{L} + \text{Mo}_{\text{SS}} \leftrightarrow \text{Mo}_3\text{Si}$ peritectic reaction. Figure 5(b) shows the XRD pattern of this alloy, where all the reflections from the Mo_3Si JCPDS standard (#4-0814) can be identified. Table 2 shows the results of EDS analyses of the four alloys whose micrographs are shown in Fig. 4(a) to (d).

The $\text{Mo}_{76}\text{Si}_{24}$, $\text{Mo}_{75}\text{Si}_{25}$, and $\text{Mo}_{74}\text{Si}_{26}$ alloys presented only the phases Mo_3Si and Mo_5Si_3 in their microstructures, confirmed by the XRD data (Fig. 5c) and EDS analysis (Table 2). Figure 4(c) shows a micrograph from the $\text{Mo}_{74}\text{Si}_{26}$ alloy. The microstructures suggested that the Mo_3Si phase is primary in all of them; however, the previous discussion concerning a possible formation and dissolution of primary Mo_{SS} , most likely in the $\text{Mo}_{76}\text{Si}_{24}$ and $\text{Mo}_{75}\text{Si}_{25}$ alloys, should be kept in mind. The most significant finding in the case of these alloys was the clear observation of the eutectic reaction involving the Mo_3Si and Mo_5Si_3 phases, as can be observed in Fig. 4(c). As expected, among the three alloys compositions, the $\text{Mo}_{74}\text{Si}_{26}$ alloy presented the largest volume of eutectic regions.

The $\text{Mo}_{73}\text{Si}_{27}$, $\text{Mo}_{72}\text{Si}_{28}$, and $\text{Mo}_{71}\text{Si}_{29}$ alloys presented the Mo_3Si and Mo_5Si_3 phases in their microstructures. All

Table 2 Results of EDS analysis of as-cast Mo-Si alloys produced in this work

Alloy composition (at.%)	Phase	Mo (at.%)	Si (at.%)
$\text{Mo}_{79}\text{Si}_{21}$	Mo_{SS}	93.0	7.0
	Mo_3Si	80.9	20.1
$\text{Mo}_{77}\text{Si}_{23}$	Mo_{SS}	93.2	6.8
	Mo_3Si	80.2	19.8
$\text{Mo}_{74}\text{Si}_{26}$	Mo_3Si	79.5	20.5
	Mo_5Si_3	66.9	33.1
$\text{Mo}_{73}\text{Si}_{27}$	Mo_3Si	79.2	20.8
	Mo_5Si_3	66.8	33.2

of them showed nonfaceted primary dendrites of the Mo_5Si_3 phase and a eutectic microstructure formed by the Mo_3Si and Mo_5Si_3 phases in the interdendritic region. As expected, the amount of Mo_5Si_3 -phase primary increases in the following order: $\text{Mo}_{73}\text{Si}_{27}$, $\text{Mo}_{72}\text{Si}_{28}$, and $\text{Mo}_{71}\text{Si}_{29}$. Figure 4(d) shows a micrograph from the $\text{Mo}_{73}\text{Si}_{27}$ alloy and Fig. 5(d) its XRD pattern. The EDS analysis results are shown in Table 2. As can be noted, the results from the $\text{Mo}_{74}\text{Si}_{26}$ and $\text{Mo}_{73}\text{Si}_{27}$ alloys confirm that the liquid eutectic composition associated with the $\text{L} \leftrightarrow \text{Mo}_3\text{Si} + \text{Mo}_5\text{Si}_3$ reaction is located between 26 and 27 at.% Si, as proposed by Svechnikov *et al.* [1971Sve].

Conclusions

Based on the microstructural analysis of several arc-melted Mo-Si alloys, it was possible to evaluate the invariant reactions involving the liquid phase in the Mo-rich portion of the Mo-Si system. The results have shown clearly the existence of a eutectic reaction involving the phases Mo_3Si and Mo_5Si_3 , indicating the existence of the $\text{L} + \text{Mo}_{\text{SS}} \leftrightarrow \text{Mo}_3\text{Si}$ and $\text{L} \leftrightarrow \text{Mo}_3\text{Si} + \text{Mo}_5\text{Si}_3$ reactions. In addition, alloys with compositions 26 at.% Si and 27 at.% Si presented Mo_3Si and Mo_5Si_3 as primary phases, respectively, indicating that the liquid eutectic composition is located between 26 and 27 at.% Si.

References

- 1952Kie:** R. Kieffer and E. Cerwenka: *Z. Metallkd.*, 1952, vol. 43, pp. 101-05.
- 1954Now:** H. Nowotny, E. Parthe, R. Kieffer, and F. Benesovsky: *Monatsh. Chem.*, 1954, vol. 85, pp. 255-72.
- 1955Aro:** B. Aronson: *Acta Chem. Scand.*, 1955, vol. 9, pp. 1107-10.
- 1956Dau:** C.H. Dauben, D.H. Templeton, and C.E. Meyers: *J. Phys. Chem.*, 1956, vol. 60, pp. 443-45.
- 1960Amb:** S. Amberg: *Monatsh. Chem.*, 1960, vol. 91, pp. 412-25.
- 1971Sve:** V.N. Svechnikov, Y.A. Kocherzhinskii, and L.M. Yupko: *Diagrammy Sostoyaniya Metal Sist. Nauka*, 1971, pp. 116-19.
- 1983Chr:** A.N. Christensen: *Acta Chem. Scand.*, 1983, vol. A37, pp. 519-22.
- 1985Arp:** E. Arpacı and M.G. Froberg: *Z. Metallkd.*, 1985, vol. 76 (6), pp. 440-44.
- 1991Gok:** A.B. Gokhale and G.J. Abbaschian: *J. Phase Equilibria*, 1991, vol. 12 (4), pp. 493-98.